ACTA ORTHOPAEDICA et TRAUMATOLOGICA TURCICA
www.aott.org.tr

Research Paper

The effect of endostatin on angiogenesis and osteogenesis of steroid-induced osteonecrosis of the femoral head in a rabbit model

Yan Zhao[1], Dong Li[1], Da-Peng Duan[2], Qi-Chun Song[1]

[1]*Department of Orthopaedics, The Second Affiliated Hospital of Xi'an Jiaotong University, Xi'an, Shaanxi Province, P.R. China*
[2]*Department of Orthopaedics, The Third Affiliated Hospital of Xi'an Jiaotong University, Shaanxi Provincial People's Hospital, Xi'an, Shaanxi Province, P.R. China*

ARTICLE INFO

Article history:
Submitted June 18, 2021
Received in revised form
September 16, 2021
Last revision received
April 16, 2022
Accepted April 29, 2022

Keywords:
Osteonecrosis of the femoral head
Endostatin
Vascular endothelial growth factor
Angiogenesis
Osteogenesis

ORCID iDs of the authors:
Y.Z. 0000-0002-3934-2871;
D.L. 0000-0002-6615-0621;
D-P.D. 0000-0001-6532-5154;
Q-C.S. 0000-0003-2111-5037.

ABSTRACT

Objective: This study aimed to investigate whether endostatin, a crucial anti-angiogenic factor, plays a negative role in angiogenesis and osteogenesis and aggravates the progression of osteonecrosis of the femoral head induced by steroid use in a rabbit model.

Methods: 66 New Zealand white rabbits were randomly divided into four groups: glucocorticoid model (GC) group (GC group, n = 18), glucocorticoid model and endostatin group (GC&ES group, n = 18), ES group (ES group, n = 18), and blank control group (CON group, n = 12). In the GC group, 10 μg/ kg lipopolysaccharide (LPS) was intravenously injected into the ear margin, and 24h after LPS injection, 20 mg/kg GC methylprednisolone (MPS) was injected into the gluteus muscle three times, each time at an interval of 24h. The animals of the GC&ES group were given as same treatment as the GC group, except for the addition of ES. MPS was not used in the ES group and CON group. ES group was only given ES, while the CON group was only given the same amount of normal saline. All animals successfully established models of femoral head necrosis, and then the difference among the Immunohistochemistry, Quantitative polymerase chain reaction (qPCR) analysis, Enzyme-linked immunosorbent assay, Biomechanical test, etracycline-calcein double labeling, and Van Gieson staining indices were compared among the four groups.

Results: The combination of MPS and LPS was successful in establishing the femoral head necrosis model in New Zealand white rabbits. The incidence of osteonecrosis after MPS and LPS intervention was 70% (7/10), while that plus ES was 100% (10/10). At the same time, after MPS and LPS intervention, while the empty bone lacuna rate of the femoral head was significantly increased, the number of osteoblasts was decreased. Also, the expressions of CD31 positive cells, Runx2, Osterix, COL1A1, and VEGF mRNA in the femoral head were decreased, and the levels of osteogenesis-related protein b-ALP, OCN, and angiogenic factor VEGF in the femoral head were decreased. The percentage of the trabecular bone area (%Tb.Ar), trabecular thickness (Tb.Th), trabecular number (Tb.N), labeled perimeter percent (%L.Pm), mineral apposition rate (MAR), and bone formation rate (BFR/BS) in the femoral head after MPs and LPS intervention detected by tetracycline calcein double labeling and Van Gieson staining decreased significantly, except trabecular separation (Tb.Sp) increased significantly. The compressive strength (CS), elastic modulus (EM), and strain energy (SE) of the femoral head examed by biomechanical measurement decreased significantly. All the above changes were more obvious after adding ES intervention. ES mRNA in the femoral head was undifferentiated and increased in the GC, ES, and GC&ES group compared with group CON.

Conclusion: This study has revealed that ES can inhibit angiogenesis and osteogenesis in the femoral head and aggravate the occurrence and development of femoral head necrosis. Thus, antiangiogenic factors may play an important role in the pathogenesis of ONFH.

Introduction

Non-traumatic osteonecrosis of the femoral head (ONFH) is a serious disease, and early intervention is an effective treatment. Patients with ONFH are often disabled because of late joint destruction, and total hip replacement is often performed to treat late necrosis of the femoral head.[1] However, the exact etiology and pathogenesis of ONFH, which is related to bone cell apoptosis, vascular injury, intravascular coagulation, dyslipidemia, increased intraosseous pressure, and immune function disorder, remain unclear.[2-5] In addition, tissue ischemia leads to necrosis of bone cells and bone marrow cells and then to ONFH.[6] During the process, the necrotic site is accompanied by bone repairment.[7,8] Tissue repair failure aggravates the necrosis and eventually causes cystic degeneration, sclerosis, and collapse of the femoral head.[9]

Bone tissue repair is closely related to angiogenesis, and impaired angiogenesis can lead to tissue repair failure.[9,10] Angiogenesis in tissue is regulated by many active factors, including proangiogenic and anti-angiogenic factors, which makes angiogenesis orderly.[11-14] Angiogenesis dysregulation leads to tissue repair failure.[15,16] Vascular endothelial growth factor (VEGF) is the most studied and the most active angiogenic factor,[17] and it exerts a certain therapeutic effect on femoral head necrosis.[18,19] Meanwhile, endostatin (ES) is the most widely studied and the most active endogenous anti-angiogenic factor, and it is used as an anti-tumor drug in clinical settings.[20,21] An imbalance in the expression of VEGF and ES leads to the development of many diseases.[22-25] Many studies suggested that vascular endothelial injury plays a key role in the pathogenesis of ONFH, and angiogenesis disruption leads to bone repair failure in the necrotic area of the femoral head and then to

Corresponding author:
Qi-Chun Song
qichuns@xjtu.edu.cn

Cite this article as: *Zhao Y, Li D, Duan D, Song Q. The effect of endostatin on angiogenesis and osteogenesis of steroid-induced osteonecrosis of the femoral head in a rabbit model. Acta Orthop Traumatol Turc. 2022;56(3):178-186.*

DOI: 10.5152/j.aott.2022.21248

osteonecrosis (ON).[19,26] Promoting angiogenesis can improve bone repair and exert a therapeutic effect on ONFH.[27,28]

Endostatin can inhibit the proliferation and migration of vascular endothelial cells by blocking the receptor of VEGF, thus inhibiting angiogenesis, VEGF secretion, and vascularization of vascular endothelial cells.[29] It can also inhibit the osteogenesis of osteoblasts.[30] Many cases of ON of the femur and tibia are caused by bevacizumab, another anti-angiogenetic factor used to treat certain types of cancer.[31] Therefore, ES may play an important negative role in femoral head necrosis. Many studies have shown the beneficial effect of VEGF on femoral head necrosis, but the negative effect of ES on femoral head necrosis has not been verified.

This study aimed to establish steroid-induced femoral head necrosis in New Zealand white rabbits and investigate the negative effects of ES on the angiogenesis and osteogenesis of glucocorticoid (GC)-induced ONFH.

Materials and Methods

Animals and grouping

The experimental protocol was approved by the Institutional Animal Use and Care Review Board of Xi'an Jiaotong University. Sixty-six adult female New Zealand white rabbits (weight: 3.2 ± 0.55 kg; age: 28 weeks) were investigated. All rabbits were housed at the Animal Centre of Xi'an Jiaotong University and maintained on a standard laboratory feeding in separate cages with a day/night cycle of 12 h light/12 h dark, a temperature of 18°C-25°C, and a humidity of 40-60%.

The 66 New Zealand white rabbits were randomly divided into 4 groups as follows: a glucocorticoid model group (GC group, n=18), a glucocorticoid model and endostatin group (GC&ES group, n=18), an ES group (ES group, n=18) and a blank control group (CON group, n=12). No significant difference in body weight was found among the 4 groups ($P > .05$). In the GC group, 10 μg/kg lipopolysaccharide (LPS; Pfizer Inc., NY, USA) was intravenously injected into the ear margin. At 24 hours after LPS injection, 20 mg/kg GC methylprednisolone (MPS) (Pfizer Inc.) was injected into the gluteus muscle for 3 times at 24 hours intervals. During MPS injection, 400 000 U penicillin (Huabei Inc., Shijiazhuang, China) was injected intraperitoneally to every animal daily to prevent infection. The animals in the GC&ES group received the same treatment as those in the GC group plus ES. Methylprednisolone was not used in the ES and CON groups. The animals in the ES group only received ES, whereas those in the CON group only received the same amount of normal saline. All animals were sacrificed by injecting excessive 10% chloral hydrate via the ear vein 6 weeks after the last injection of MPS.

Recombinant human ES (Simcere Medgenn, Nanjing, China) injection was performed as previously described.[32] A 2 mg/kg dose of ES was subcutaneously injected. Results of a pre-experiment confirmed that this dose exerts no obvious adverse reaction on animals and inhibits the expression of serum VEGF (enzyme-linked immunosorbent assay, ELISA). The animals in the GC&ES and ES groups were treated once a day for 6 weeks from the day before modeling, whereas those in the GC and CON groups only received the same amount of normal saline.

Specimen collection and preparation

The 66 rabbits were divided into 2 parts composed of 42 and 24 rabbits. The 42 rabbits were used for immunohistochemistry, quantitative polymerase chain reaction (qPCR) analysis, ELISA, and other analyses. Six rabbits were randomly selected from the CON group, and 12 rabbits were randomly selected from the 3 other groups (GC group, n=12; GC&ES group, n=12; ES group, n=12; CON group, n=6). Animals were fasted for 12 hours before sacrifice, and 2 mL of venous blood was collected through the ear vein and injected into a centrifuge tube without an anti-coagulant, which was placed at room temperature for 2 hours. The supernatant was centrifuged at 2000 rpm for 10 minutes, transferred to a new centrifuge tube, and then stored at −20°C for experimental purposes. Bilateral femoral heads were collected immediately after death. The left femoral head was divided into 2 parts along the sagittal plane. One part was immediately fixed with 10% neutral formaldehyde for 3 days and then decalcified in 10% ethylenediamine tetraacetic acid (EDTA) decalcifying solution. The specimen was waxed, embedded, and then sectioned into 5-μm-thick slices until further use. The other part was quickly stored in a −20°C refrigerator until PCR detection. Two pieces of bone were obtained from the right femoral head according to the gravity direction of the femoral head, and the length was measured with a vernier caliper. One piece was a 4 mm × 4 mm × 3 mm subchondral bone plate, and the other piece was a 6 mm × 6 mm × 6 mm cancellous bone in the middle of the femoral head. Normal saline was continuously used to wet the tissue block, and the direction of loading was indicated. The tissue block was stored at −20°C for biomechanical determination.

The other 24 rabbits were used for morphometric determination (GC group, n=6; GC&ES group, n=6; ES group, n=6; CON group, n=6). Tetracycline (TET, 8 mg/kg) (Xi'an Chemical Reagent Factory, China) was injected intramuscularly 13 days before sacrifice, and then calcein (50 mg/kg) (Xi'an Chemical Reagent Factory, China) was injected intramuscularly 3 days before sacrifice. The femoral heads of the sacrificed animals were obtained for TET calcein double labeling and Van Gieson (VG) staining.

Assessment of osteonecrosis of the femoral head

A 4-μm-thick section of each femoral head was cut in the coronal plane and stained with hematoxylin and eosin (HE). The presence or absence of ONFH was determined in whole areas of 2 sections for each rabbit. The sections were examined by 2 blinded pathologists using light microscopy (Nikon YS100; Nikon Corporation, Tokyo, Japan). Osteonecrosis of the femoral head was identified based on

HIGHLIGHTS

- Studies have shown the beneficial effect of VEGF on femoral head necrosis, but the negative effect of Endostatin (ES) on femoral head necrosis has not been verified.
- This study aimed to establish steroid-induced femoral head necrosis in New Zealand white rabbits and investigate the negative effects of ES on the angiogenesis and osteogenesis of glucocorticoid (GC)-induced osteonecrosis (ON) of the femoral head.
- The rate of ON was 70% (7/10) in the GC group, 100% (10/10) in the GC&ES group, 41.7% (5/12) in the ES group, and 0 (0/6) in the CON group. Addition of ES increased the occurence and development of GC-induced ON of the femoral head, which was also assessed by the decreased CD31 expression, RT-PCR and ELISA parameters, bone morphometric testing results and as well as biomechanical testing outcomes.
- The results of this study suggest that ES can inhibit angiogenesis and osteogenesis in the femoral head and aggravate the occurrence and development of femoral head necrosis, suggesting that anti-angiogenic factors may play an important role in the pathogenesis of ONFH.

the presence of empty lacunae or pyknotic osteocyte nuclei in the bone trabeculae and the presence of necrosis in the surrounding bone marrow or fat cells.[33] It was not classified as ONFH when empty lacunae in the bone trabeculae were present but bone marrow or fat cell necrosis was absent. Rabbits were considered to have ON when ONFH was identified in at least 1 of the 2 sections analyzed. The incidence of ON was calculated as the ratio of the number of rabbits with ONFH to the total number of rabbits. Image-Pro Plus 6.0 was used for analysis. We randomly selected 10 trabecular bone fields at a magnification of 200, counted 50 bone lacunae continuously, and calculated the rate of empty bone lacunae. The number of osteoblasts in trabecular bone was measured as the average number of osteoblasts per 1 mm of trabecular surface length.

Immunohistochemistry

Immunohistochemistry was performed using a 4-μm-thick section of each femoral head to assess the presence of CD31 using specific antibodies in accordance with the manufacturer's instructions. In brief, deparaffinized sections were treated with 3% hydrogen peroxide for 20 minutes to inhibit endogenous peroxidase activity. Antigen retrieval was then performed using 0.01 M citrate buffer (pH 6.0) at 80°C for 10 minutes. The sections were pre-incubated with normal goat serum (Biosynthesis Biotechnology Co. Ltd., Beijing, China) for 30 minutes at room temperature, incubated at 4°C overnight with mouse anti-rabbit CD31 (ab212712; Abcam PLC, Cambridge, Mass, USA) monoclonal antibodies and then diluted at 1:200 in phosphate-buffered saline. The sections were then incubated with secondary goat anti-mouse antibodies (Biosynthesis Biotechnology Co. Ltd.) and with horseradish peroxidase-labeled streptavidin (Biosynthesis Biotechnology Co. Ltd.). The final reaction product was visualized using diaminobenzidine. Images were captured using the QWin550CW Image Acquiring and Analysis system (Leica Microsystems, Wetzlar, Germany). The intensity of CD31 immunostaining in the groups was quantitatively analyzed using Image-Pro Plus (Media Cybernetics, Baltimore, Md, USA). One section was obtained from each rabbit, and 10 images were captured from each section and analyzed for positive staining at a magnification of 200×. The total area of each analyzed section was the same. Integrated optical density (IOD) was assessed, in which "integrated" refers to the sum of all the pixel intensity or density values in each image. The IOD values obtained from the 10 images in each section were averaged and compared with the averaged IOD values of each section.

qPCR analysis

Total RNA was isolated by homogenizing the femoral heads using the TRIzol® protocol. cDNA was synthesized using the RevertAid™ First Strand cDNA Synthesis kit (Fermentas, Burlington, ON, Canada) in accordance with the manufacturer's instructions. The samples were analyzed using SYBR-Green® PCR Master mix (DRR820S; Takara Bio, Inc., Shiga, Japan) and an ABI 7300 Real-Time PCR system (Bio-Rad Laboratories, Hercules, Calif, USA). The primer sequences used for qPCR were as follows: forward: 5′-GGGGGCTG CTGCAATGATGAAA-3′ and reverse: 5′-GCTGGCCCTGGTGAGGT TTGAT-3′ for VEGF; forward: 5′-TGGGGCTGGCGGGCACCTTC-3′ and reverse: 5′-TCTCGGTCAGCCTGCGCCCG-3′ for ES; forward: 5′-GTGGTGGCAGGTAGGTATGG-3′ and reverse: 5′-GGCAGGTG CTTCAGAACTGG-3′ for Runx2; forward: 5′-TGAGCTGGAACGTC ACGTGC-3′ and reverse: 5′-AAGAGGAGGCCAGCCAGACA-3′ for Osterix; forward: 5′-CTCAGGGTTTCAGTGGTT-3′ and reverse: 5′-TTTCCACGAGCACCCATC-3′ for Col1a1; and forward: 5′-GTG CGGGACATCAAGGAGA-3′ and reverse: 5′-AGGAAGGAGGGCTG GAAGAG-3′ for β-actin. Relative mRNA expression was quantified using the $2^{-\Delta\Delta Ct}$ method, in which $\Delta\Delta Ct = (Ctgene\text{-}Ct\beta)A/B/C\text{-}(Ctgene\text{-}Ct\beta)N$. The relative quantities of VEGF, ES, Runx2, Osterix, and Col1a1 were normalized to the quantity of the β-actin transcript in the same sample. All assays were performed in triplicate.

Enzyme-linked immunosorbent assay

Prior to sacrifice, blood was collected from all rabbits with a mixture of protease inhibitors (0.30 M EDTA, 0.32 M dimercaprol, and 0.34 M 8-sulfhydryl quinoline sulfate) and then stored on ice. Blood was then centrifuged at 2000 rpm for 10 minutes. The plasma was obtained and stored at −80°C until use for VEGF, osteocalcin (OCN), and beta-alkaline phosphatase (b-ALP) assays. The concentrations of VEGF, OCN, and b-ALP were measured using ELISA with a commercial ELISA kit (Biosynthesis Biotechnology Co. Ltd., Beijing, China). The concentrations of VEGF, OCN, and b-ALP were expressed as pg/mL plasma. All analyses were performed in duplicate.

Biomechanical test

The specimen was rewarmed at room temperature, and the bone block was pressed with an MTS-858 biomaterial testing machine at a set speed of 5 mm/min. The subchondral bone was compressed with a round indenter with a diameter of 2 mm. The compression strength (CS) was the ratio of the pressure to the area of the indenter, and the elastic modulus (EM) was the average slope of the same range. The cancellous bone was loaded according to Brown's loading method. The area under the stress–strain curve from the beginning to 0.8 strain was calculated, and then the strain energy (SE) at 0.8 compression strain was calculated according to the area. The CS and EM were expressed in MPa, and the SE was expressed in MJ/mm^2.

TET calcein double labeling and Van Gieson staining

The prepared femoral head specimens were embedded with plastic embedding. The hard tissue embedded block was properly trimmed and sectioned with a slicer (Leica 2500e, Leica Company). Then, 10-μm-thick hard tissue sections were observed under a 200-fold fluorescence microscope, and fluorescence bands with clear lines and complete shapes were selected for photography. The distance between the 2 fluorescent bands was measured using IPP 5.1 image analysis software (Media Cybernetics, USA). Dynamic parameters including labeled perimeter percentage (L.Pm%), mineral deposition rate (MAR, μm/day), and bone formation rate (BFR/BS, %) were calculated.

Then, 5-μm-thick hard tissue sections were stained with VG. They were observed under an inverted microscope and randomly photographed at a magnification of 100×. IPP 5.1 image analysis software (Media Cvbemetrics) was used. Static parameters including trabecular bone area, trabecular thickness (Tb.Th, μm), trabecular separation (Tb.Sp), and trabecular number (TB.N, #/mm) were calculated.

Statistical analysis

All statistical analyses were performed using SPSS 20.0 (IBM SPSS Corp., Armonk, NY, USA). The incidence of ON was compared using the χ^2 test or Fisher's exact test. Data were expressed as mean ± standard deviation and compared using the 1-way analysis of variance or Kruskal–Wallis test. Statistical significance was considered at $P < 0.05$.

Results

Incidence of osteonecrosis of the femoral head

In this study, 2 animals each in the GC and GC&ES groups died; no animals in the other groups died. The rate of ON was 70% (7/10) in the GC group, 100% (10/10) in the GC&ES group, 41.7% (5/12) in the ES group, and 0 (0/6) in the CON group. The incidence rates of the GC&ES and GC groups were higher than that of the ES group ($P <$ .05). No significant difference in incidence rate was found between the GC&ES and GC groups ($P >$.05, Pearson's chi-square test), but the incidence rate was higher in the GC&ES group than in the GC group. Histological features of ON in the femoral head of the rabbits showed condensed nuclei of osteocytes or empty lacunae within the bone trabeculae and decreased osteoblasts in the trabecular margin; medullary hematopoietic cells around the ON site were mixed with necrotic and degenerated cells, and necrotic fat cells lost their cellular structures (Figures 1A–C). However, normal bone tissue harvested from the CON group showed no ON (Figure 1D). The rates of empty bone lacunae were higher in the GC and ES groups than in the CON group, but that in the GC&ES group was significantly higher than that in the GC or ES group ($P <$ .05; Figure 1E). Compared with that in the CON group, the number of osteoblasts in the GC, ES, and GC&ES groups was significantly lower ($P <$ .05), especially in the GC&ES group. Significant differences were found between the ES and GC groups ($P <$ .05; Figure 1F).

CD31 expression in bone

In the 200× field of vision, the brown staining in the trabecular bone was CD31 positive, and any single or clustered endothelial cells could be counted as a single vessel. Compared with that in the CON group (n = 6), the number of microvessels in the GC (n = 10), ES (n = 12), and GC&ES (n = 10) was significantly lower ($P <$ .05), especially in the GC&ES group (Figure 2).

Real-time quantitative PCR results

As shown in Figure 3A, the VEGF mRNA expression was lower in the GC group (n = 10) and ES group (n = 12) than in the CON group (n = 6; $P < 0.05$) and decreased more obviously in the GC&ES group than in the GC and ES groups. As shown in Figure 3B, the ES mRNA expression in the femoral head increased in the GC, ES, and GC&ES groups compared with the CON group. As shown in Figure 3C–E, the expression levels of bone-generating related genes Runx2, Osterix, and Col1a1 significantly decreased in the GC and ES groups compared with the CON group ($P < 0.05$), but the decrease in these genes (except Col1a1) was more significant in the GC&ES group than in the GC and ES groups ($P < 0.05$).

Bone morphometric determination results

All animals in each group (n = 6) applied for bone morphometric determination survived. As shown in Figure 4, the fluorescence signals in the GC group (n = 6) and the ES group (n = 6) were significantly lower than those in the CON group (n = 6) and the gap between calcein fluorescence (green) and TET fluorescence (yellow) was significantly narrower in the GC and ES groups than in the CON group. Combined GC and ES intervention enhanced the effect of GC. The fluorescence intensity was weaker and the gap between calcein fluorescence (green) and TET fluorescence (yellow) was narrower in the ES group than in the CON group. Bone morphometric

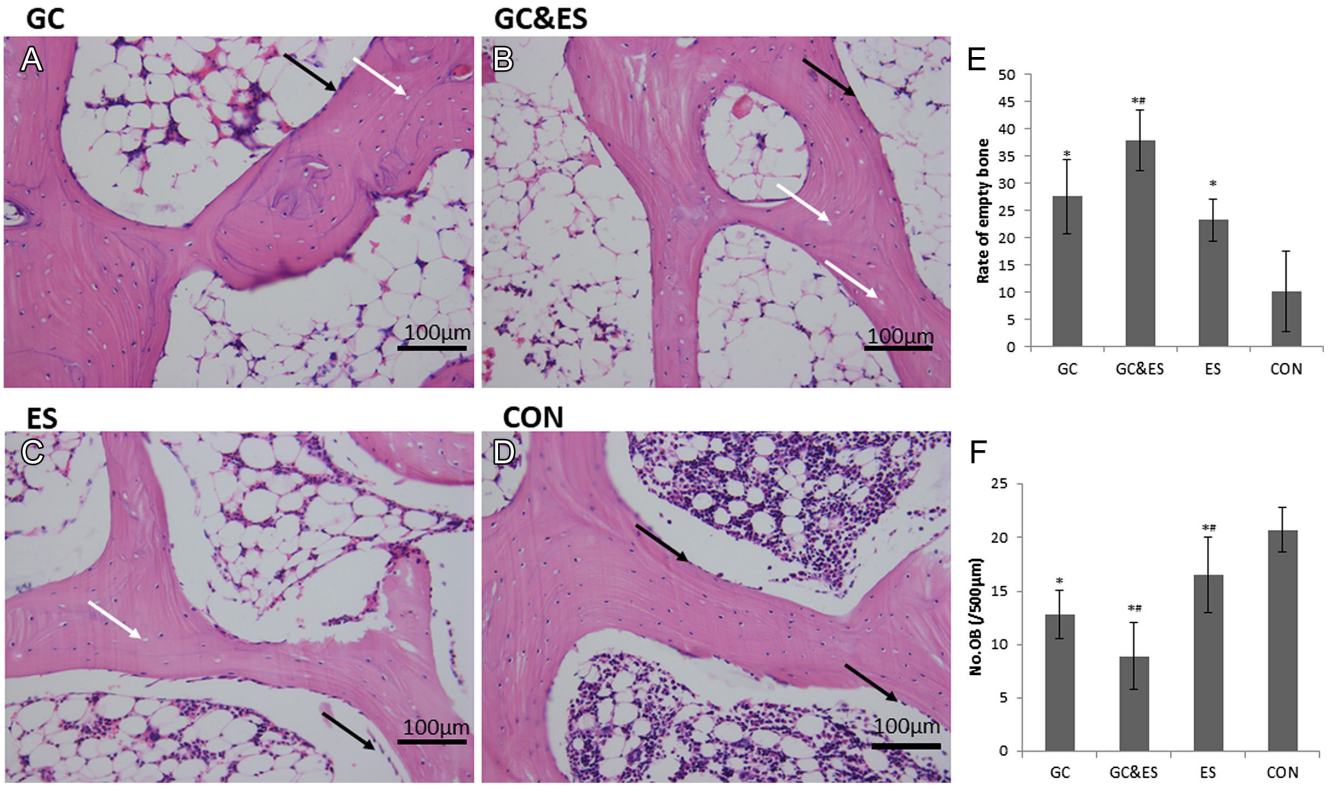

Figure 1. A-F. Histological features of the femoral head in rabbits. (A, B, and C) Osteonecrotic (ON) lesion condensed nuclei of osteocytes or empty lacunae within the bone trabeculae (white arrow) and decreased osteoblasts in the trabecular margin *(*black arrow). Medullary hematopoietic cells around the site of ON were mixed with necrotic and degenerated cells, and necrotic fat cells lost their cellular structures. (D) Normal bone tissue harvested from group CON showing no ON. Stain: hematoxylin and eosin (H&E), magnification: ×200. (E) The rate of empty bone lacunae was increased in the GC group and ES group, and the increase in the GC&ES group was more obvious. (F) The number of osteoblasts in GC or ES groups decreased, and the decrease in GC&ES group was more obvious. *Compared with CON group, $P < 0.05$; #compared with GC group, $P <$.05. GC, glucocorticoid; ES, endostatin; CON, control.

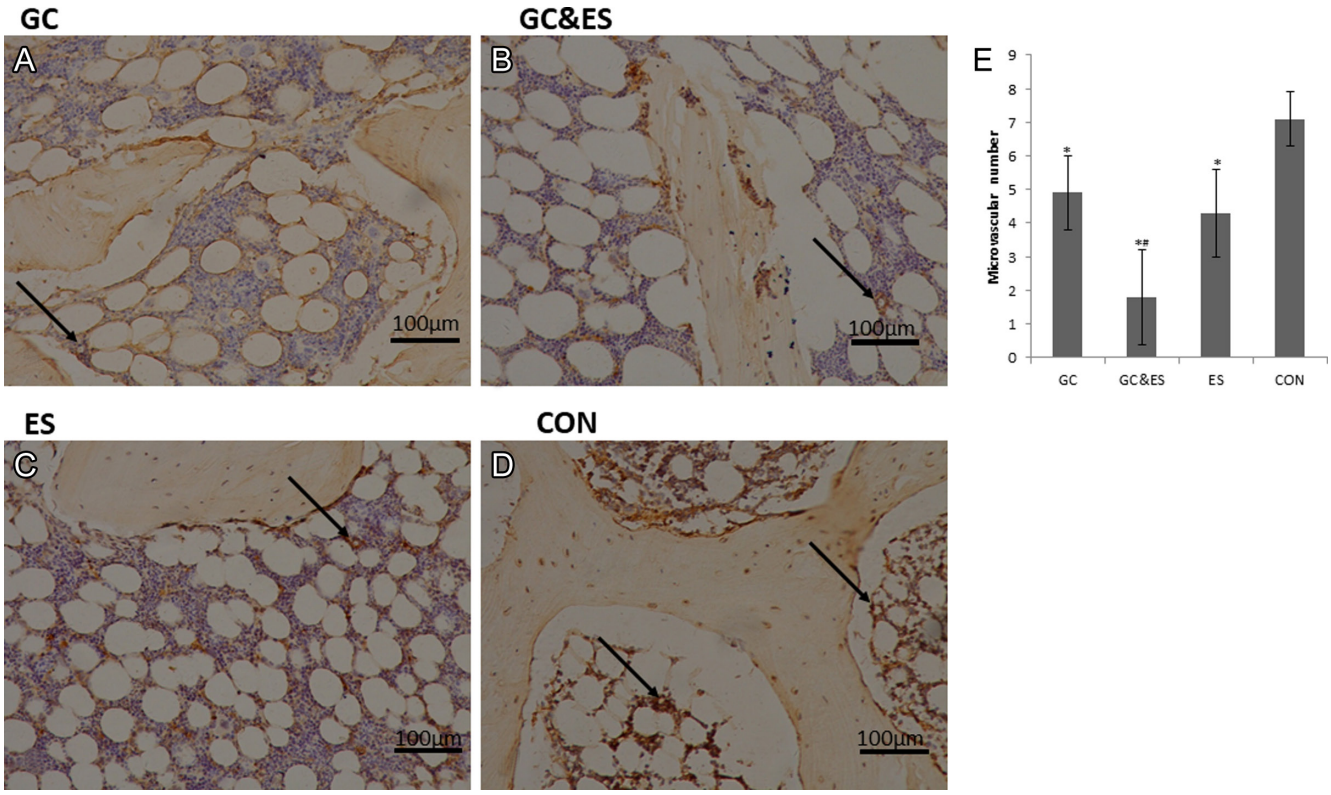

Figure 2. A-E. CD31 expression in the femoral head of rabbits. In the GC group and ES group, there were very few brown stained CD31 positive vessels (A and C), fewer positive vessels in GC&ES group (B), but more CD31 positive vessels in the CON group (D). Any single or clustered endothelial cells could be counted as a single vessel (black arrow). (E) The number of microvessels in each group was compared. The microvascular number was decreased in the GC group and ES group, which in the GC&ES group was decreased more obviously. *Compared with CON group, $P < 0.05$; #compared with GC group, $P < 0.05$. GC, glucocorticoid; ES, endostatin; CON, control.

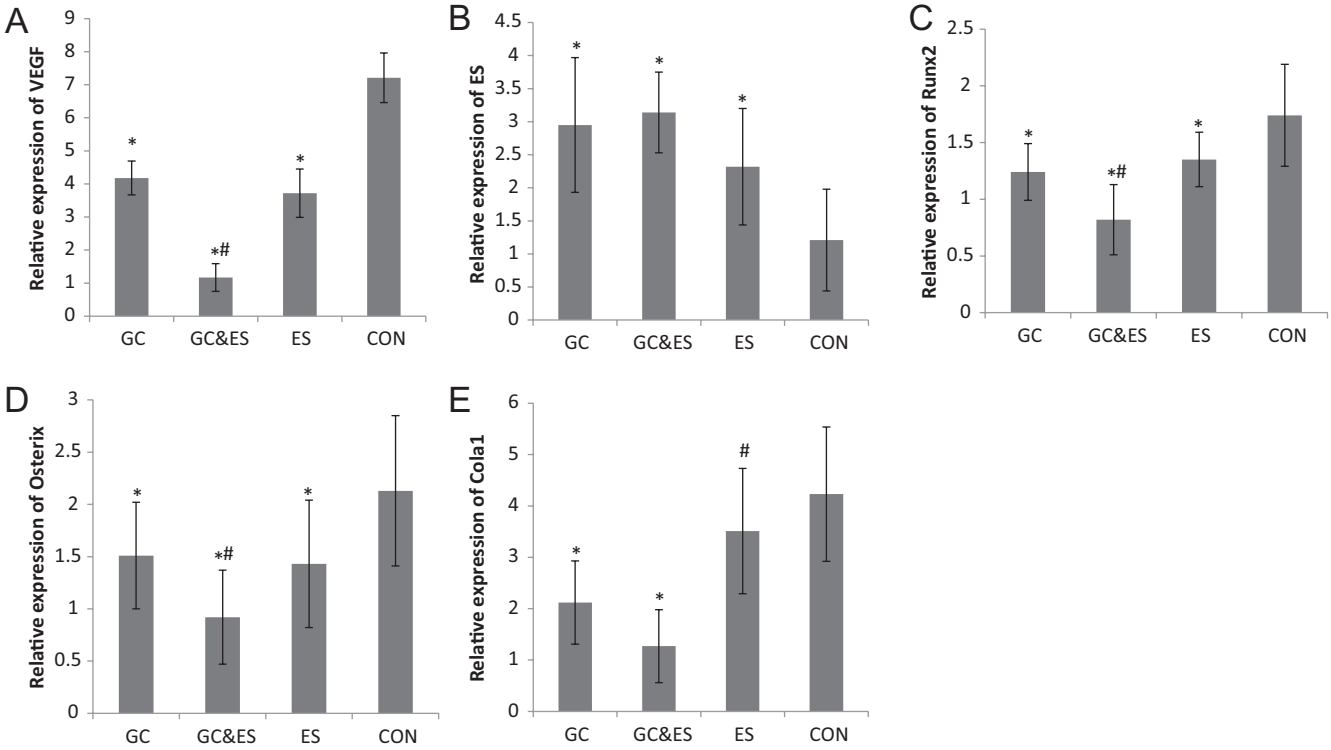

Figure 3. A-E. (A) Expression of VEGF mRNA, (B) ES mRNA, (C) Runx2 mRNA, (D) Osterix mRNA, and (E) Col1a1 mRNA in each group. *Compared with CON group, $P < 0.05$; #compared with GC group, $P < 0.05$. GC, glucocorticoid; ES, endostatin; CON, control; VEGF, Vascular endothelial growth factor.

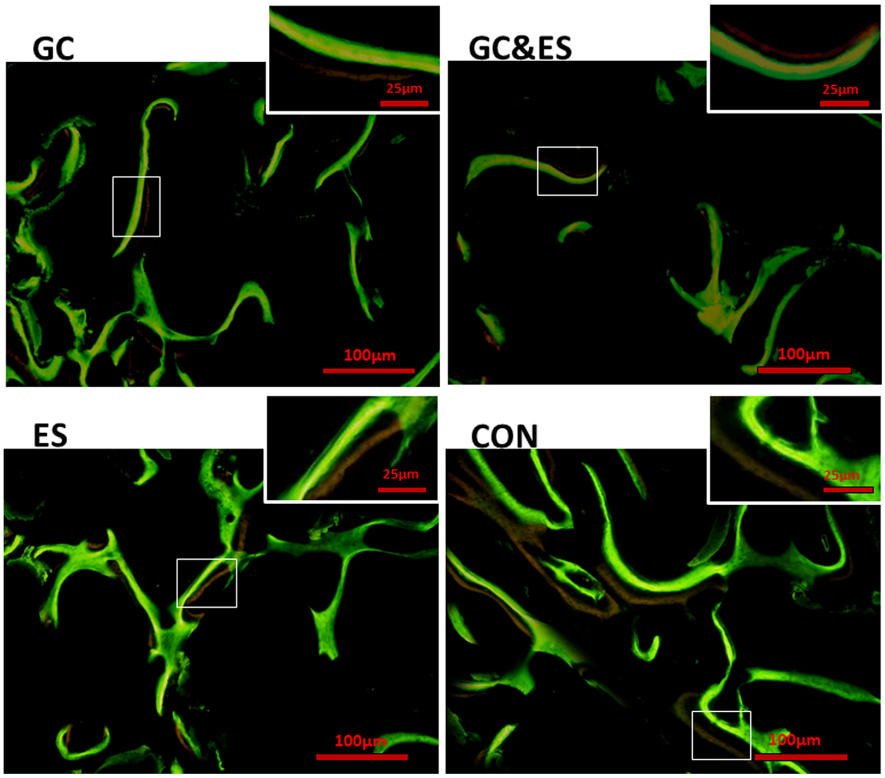

Figure 4. Dynamic bone formation was detected by calcein tetracycline double labeling. GC, GC&ES, ES, and CON are the double labeling conditions of each group, respectively. The fluorescence intensity and the width between yellow and green fluorescence represent the capability of bone formation. The small picture in the upper right corner is the enlargement in the white box of the large picture to observe the width between yellow and green fluorescence. GC, glucocorticoid; ES, endostatin; CON, control.

determination showed that the L.pm%, MAR, and BFR/BS of the GC, ES, and GC&ES groups, especially those of the GC&ES group, were significantly lower than those of the CON group ($P < 0.05$). Labeled perimeter percentage and MAR were significantly different between the GC and ES groups ($P < 0.05$), but no significant difference in BFR/BS was found between the 2 groups ($P > 0.05$; Table 1).

The trabecular bone stained with VG appeared red (Figure 5). Compared with that of the CON group, the bone mass values of the GC&ES, GC, and ES groups were significantly lower ($P < 0.05$), especially in the GC&ES group ($P < 0.05$). Static parameters related to bone morphometry, including BV/TV, Tb.Th, Tb.Sp, and Tb.N, were analyzed to accurately compare the changes in bone mass in each group. Compared with those in the control group, the BV/TV and Tb.Th in the 3 other groups, especially in the GC&ES group, were significantly lower ($P < 0.05$). No significant difference in Tb.N was found among the 4 groups ($P > 0.05$), but they had the same trend as BV/TV and Tb.Th. Conversely, an opposite trend was observed in Tb.Sp. (Table 2).

ELISA results

The serum levels of VEGF, b-ALP, and OCN were detected using ELISA. Compared with those in the CON group (n=6), the VEGF, b-ALP, and OCN levels were significantly lower in the GC (n=10), ES (n=12), and GC&ES (n=10) groups, especially in the GC&ES group ($P < 0.05$). The serum levels of b-ALP and OCN in the ES group were still higher than those in the GS group ($P < 0.05$), but no significant difference in VEGF was found ($P > 0.05$; Table 3).

Table 1. Comparison of dynamic parameters of bone morphometric in each group (n=6/group)

Groups	L.Pm%	MAR (μm/d)	BFR/BS (μm/d.100)
GC	17.56 ± 4.07*	1.03 ± 0.17*	18.80 ± 3.11*
GC+ES	12.11 ± 3.54*♯	0.42 ± 0.07*♯	8.28 ± 1.19*♯
ES	19.59 ± 2.64*	1.46 ± 0.31*♯	24.28 ± 4.53*♯
CON	28.50 ± 5.45	1.88 ± 0.29	50.54 ± 6.52

*Compared with CON group, $P < 0.05$; ♯compared with GC group, $P < 0.05$.
GC, glucocorticoid; ES, endostatin; CON, control; L.Pm%, labeled perimeter percentage; MAR, mineral deposition rate; BFR/BS, bone formation rate.

Biomechanical test results

As shown in Table 4, compared with those in the CON group, the CS, EM, and stress energy in the GC group significantly decreased by 46.5%, 44.4%, and 47.0%, respectively; by 33.8%, 33.6%, and 41.1% in the ES group, respectively, and by 72.0%, 81.5%, and 56.8% in the GC&ES group, respectively ($P < 0.05$). Compared with those of the GC group, the CS and EM of the ES group decreased less ($P < 0.05$), but no significant difference in stress energy was found between the 2 groups ($P > 0.05$).

Discussion

The exact mechanism of non-traumatic ONFH is unclear. Thus, many types of animal models have been established to explain non-traumatic ONFH. However, a standardized and unified model remains lacking, and clinical femoral head necrosis is difficult to stimulate.[2,9] At present, non-traumatic ONFH animal models are mainly established under the premise of known etiology, including GC, alcohol, LPS, liquid nitrogen freezing, and decompression model.[6,7] Glucocorticoid is a key risk factor of ON. In this animal experiment, the animal model established by Qin et al[34] was used. This study showed a high incidence (93%) of ON and low mortality. The model used in this study had a 70% (7/10) incidence rate and low animal mortality rate, which lays a good foundation for the continuation of this experiment.

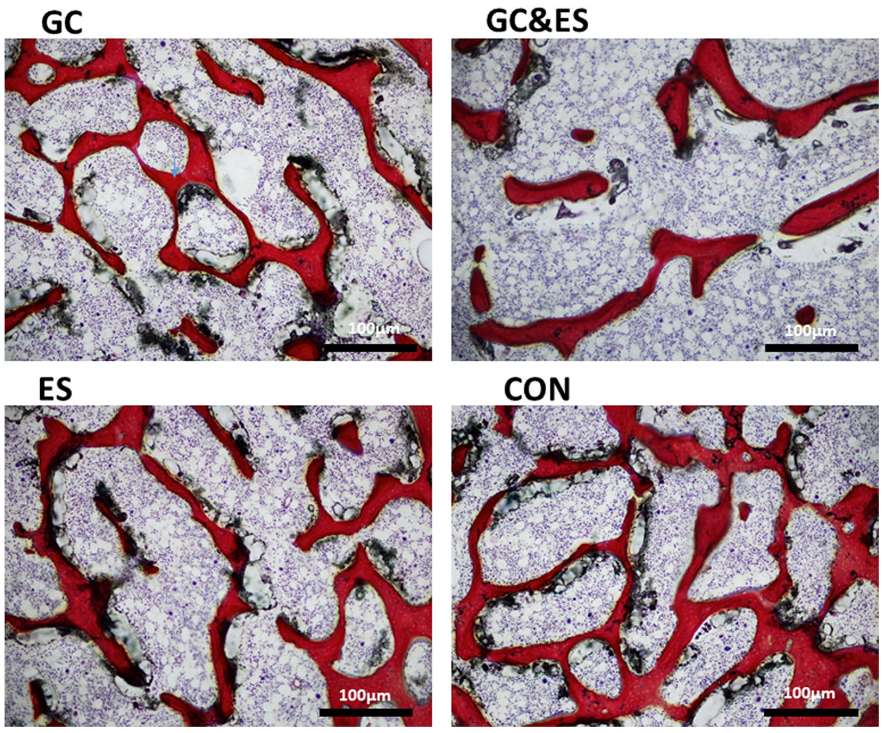

Figure 5. Static bone morphology was detected by Van Gieson staining. GC, GC&ES, ES, and CON were the staining conditions of each group. The red staining area was bone trabecula, and the grey staining area was bone marrow. GC, glucocorticoid; ES, endostatin; CON, control.

Table 2. Comparison of static parameters of bone morphometric in each group (n=6/group)

Groups	BV/TV (%)	Tb.N (#/mm)	Tb.Sp (μm)	Tb.Th (μm/d)
GC	21.55 ± 4.49*	5.25 ± 2.01	162.98 ± 32.21	44.53 ± 14.21*
GC+ES	12.21 ± 2.13*♯	5.01 ± 1. 38	189.43 ± 42.45	25.11 ± 12.31*♯
ES	30.81 ± 3.35*	5.13 ± 0.37	179.81 ± 49.95	35.34 ± 9.33*
CON	35.87 ± 6.69	5.87 ± 0.82	135.01 ± 26.32	70.82 ± 17.39

*Compared with CON group, $P < 0.05$; ♯compared with GC group, $P < 0.05$.
GC, glucocorticoid; ES, endostatin; CON, control; Tb.N, trabecular number; Tb.Sp, trabecular separation; Tb.Th, trabecular thickness.

Table 3. Comparison of serum VEGF, b-ALP, and OCN levels in each group

Groups		OCN (μg/L)	VEGF (μg/L)
GC (n=10)	47.75 ± 7.41*	26.21 ± 6.76*	46.31 ± 2.29*♯
GC&ES (n=10)	26.75 ± 3.57*♯	17.21 ± 5.71*♯	22.24 ± 4.21*♯
ES (n=12)	55.23 ± 8.43*♯	23.11 ± 2.22*♯	42.18 ± 3.43*
CON (n=6)	85.42 ± 9.01	53.12 ± 3.46	61.32 ± 6.59

*Compared with CON group, $P < 0.05$; ♯compared with GC group, $P < 0.05$.
GC, glucocorticoid; ES, endostatin; CON, control; VEGF, vascular endothelial growth factor; OCN, osteocalcin; b-ALP, beta-alkaline phosphatase.

As an endogenous anti-angiogenic factor, ES exerts anti-angiogenic properties. At present, its anti-angiogenic properties are mainly used to inhibit tumor growth.[29,32,35] Endostatin is increased in patients with coronary artery disease and is closely related to the formation of damaged coronary artery branches.[36] The decrease in ES level is an important reverse marker of collateral formation in coronary ischemic disease.[37] The above 2 studies have shown that

Table 4. Biomechanical results of femoral head

Groups	CS (MPa)	EM (MPa)	SE (mJ/mm²)
GC (n=10)	19.04 ± 3.19*	197.04 ± 76.31*	2.53 ± 0.71*
GC&ES (n=10)	9.96 ± 1.09*♯	65.67 ± 20.25*♯	2.06 ± 0.34*♯
ES (n=12)	23.56 ± 4.34*♯	235.86 ± 75.93*♯	2.71 ± 0.62*
CON (n=6)	35.58 ± 3.25	354.43 ± 96.21	4.77 ± 1.01

*Compared with CON group, $P < 0.05$; ♯compared with GC group, $P < 0.05$.
GC, glucocorticoid; ES, endostatin; CON, control; CS, compressive strength; EM, elastic modulus; SE, strain energy.

ES exhibits anti-angiogenic characteristics and its overproduction means the occurrence of ischemia. In the present study, the detection of microvessel density through immunohistochemistry and the expression of VEGF in serum and tissue showed that ES can reduce the density of blood vessels and the expression of angiogenic factors in the femoral head. Alexander et al[38] showed that ES can inhibit choroidal angiogenesis. In addition, Bai et al[39] reported that ES can inhibit retinal angiogenesis in vivo and umbilical vein endothelial cell proliferation in vitro and these processes are accompanied by a decrease in VEGF, which is consistent with the results of the present study. Joerg et al[30] used ES to intervene in the fracture model in mice and found that ES can significantly reduce the angiogenesis of bone healing site, thus affecting fracture healing. In the present study, ES increased in non-traumatic ONFH animal models and ES intervention strengthened the decrease in vascular density in the steroid-induced femoral head necrosis model.

Blood vessels are important components of bone formation during bone development and bone repair.[40] Osteogenesis plays an important role in the occurrence and development of non-traumatic ONFH, especially in the middle and late stages of bone repair.[18] Endostatin can inhibit bone formation by blocking VEGF, and it can also directly affect bone formation.[30] Sipola et al[41] established a mouse model of ectopic calcification and found that ES can reduce bone formation. They suggested that ES regulates endochondral osteogenesis in bone growth and repair. They also found that ES could inhibit the proliferation of osteoblasts induced by fluid shear stress and its upregulated factors.[42] In the present study, HE staining showed that the number of osteoblasts significantly reduced after the application of ES. In addition, PCR was used to detect bone formation-related genes Runx2, Osterix, and COL1A1, and serum determination was used to detect bone formation-related proteins b-ALP and OCN. Results showed that ES could further reduce these bone formation-related indicators, which indicated that ES could inhibit bone formation in

steroid-induced ONFH. In addition, TET calcein double labeling and VG staining were used for bone morphometry. The BFR/BS and total bone mass decreased during steroid-induced ON. In this study, the addition of ES to steroids can reduce bone mass and bone formation, indicating the negative effect of ES.

In the present study, the angiogenesis and osteogenesis in the femoral head were blocked after the application of ES alone, which eventually decreased bone quality and biological performance. This result indicated that ES alone could inhibit angiogenesis and osteogenesis, thereby confirming the negative role of ES on the occurrence and development of ON. Based on the above facts, we assume that ES-induced inhibition of angiogenesis induces ischemia of the femoral head, leading to the death of bone cells, bone marrow cells, and interstitial cells in bone tissue due to lack of blood. This phenomenon results in failure of repair and collapse of the femoral head, which opens a new direction for the future study of anti-angiogenic factors in ONFH.

This experiment has many limitations. Firstly, this study only focused on the factors related to the effect of ES on bone formation but did not analyze the factors related to bone resorption, which is also important in the repair of femoral head necrosis. Secondly, the specific mechanism by which ES inhibits angiogenesis and osteogenesis was not studied in detail, and only the changes in angiogenesis- and osteogenesis-related factors were considered. Thirdly, only 1 (i.e., ES) of many anti-angiogenic factors was studied. Thus, other anti-angiogenic factors, such as angiostatin, chondromodulin-I, platelet inhibitory factor-4, interleukin-12, matrix metalloproteinase, tissue inhibitor of metalloproteinase, and urokinase inhibitor, must be studied in the future. Finally, whether the anti-angiogenic factors secreted by cartilage in femoral head necrosis affect the progress of femoral head necrosis still needs to be discussed because the cartilage, as a nearly avascular tissue, can synthesize and secrete a large number of anti-angiogenic factors (such as chondromodulin-I).

In conclusion, ES can inhibit angiogenesis and osteogenesis in the femoral head and aggravate the occurrence and development of femoral head necrosis, suggesting that anti-angiogenic factors may play an important role in the pathogenesis of ONFH.

Ethics Committee Approval: The study was approved by the Institutional Animal Use and Care Review Board of Xi'an Jiaotong University (2014-567b).

Informed Consent: N/A.

Author Contributions: Concept - Y.Z., Q.S.; Design - Y.Z., D.D., Q.S.; Supervision - Y.Z., Q.S.; Materials - D.L., D.D.; Data Collection and/or Processing - D.L., D.D.; Analysis and/or Interpretation - D.L., D.D.; Literature Review - Y.Z., D.L.; Writing - Y.Z.; Critical Review - Q.S.

Declaration of Interests: The authors have no conflict of interest to declare.

Funding: The present study was funded by the National Natural Science Foundation of China (grant no. 82002311) and China Postdoctoral Science Foundation (grant no. 2021M692575).

References

1. Torgashin AN, Rodionova SS, Shumsky AA, et al. Treatment of aseptic necrosis of the femoral head. Clinical guidelines. Clinical guidelines. *Naučno-praktičeskaâ revmatologiâ*. 2021;58(6):637-645. [CrossRef]
2. Mont MA, Cherian JJ, Sierra RJ, Jones LC, Lieberman JR. Nontraumatic osteonecrosis of the femoral head: where do we stand today? A ten-year update. *J Bone Joint Surg Am.* 2015;97(19):1604-1627. [CrossRef]
3. Mont MA, Salem HS, Piuzzi NS, Goodman SB, Jones LC. Nontraumatic osteonecrosis of the femoral head: where do we stand today?: A 5-year update. *J Bone Joint Surg Am.* 2020;102(12):1084-1099. [CrossRef]
4. Mutijima E, De Maertelaer V, Deprez M, Malaise M, Hauzeur JP. The apoptosis of osteoblasts and osteocytes in femoral head osteonecrosis: its specificity and its distribution. *Clin Rheumatol*. 2014;33(12):1791-1795. [CrossRef]
5. Tian L, Wen Q, Dang X, You W, Fan L, Wang K. Immune response associated with toll-like receptor 4 signaling pathway leads to steroid-induced femoral head osteonecrosis. *BMC Musculoskelet Disord*. 2014;15:18. [CrossRef]
6. Assouline-Dayan Y, Chang C, Greenspan A, Shoenfeld Y, Gershwin ME. Pathogenesis and natural history of osteonecrosis. *Semin Arthritis Rheum*. 2002;32(2):94-124. [CrossRef]
7. Aaron RK. Concepts of the pathogenesis of osteonecrosis. *Tech Orthop*. 2001;16(1):101-104. [CrossRef]
8. Jones LC, Hungerford DS. The pathogenesis of osteonecrosis. *Instr Course Lect*. 2007;56(56):179-196.
9. Panin MA, Zagorodniy NV, Karchebnyi NN, Sadkov IA, Zakirova AR. Modern view on pathogenesis of non traumatic osteonecrosis. *N N Priorov J Traumatol Orthop*. 2017;2:69-75.
10. Huard J. Stem cells, blood vessels, and angiogenesis as major determinants for musculoskeletal tissue repair. *J Orthop Res*. 2019;37(6):1212-1220. [CrossRef]
11. Yamashiro DJ, Cohn SL. Angiogenesis. *Pediatr Oncol*. 2005.
12. Feige JJ, Pagès G, Soncin F. *Molecular Mechanisms of Angiogenesis*; 2014. [CrossRef]
13. Wicki A, Christofori G. *The Angiogenic Switch in Tumorigenesis; Tumor Angiogenesis*. 2008;1(4):67-88.
14. Sinkovics J Horák A. Angiogenesis, antiangiogenesis [Angiogenesis, anti-angiogenesis]. *Orv Hetil*; 1998;139(20):1269.
15. Hellsten Y, Hoier B, Gliemann L. What turns off the angiogenic switch in skeletal muscle? *Exp Physiol*. 2015;100(7):772-773. [CrossRef]
16. Printers C, Carmeliet p, jain r. Angiogenesis in health and disease. *Nat Med*. 2003;9(6):653-660.
17. Veikkola T, Alitalo K. VEGFs, receptors and angiogenesis. *Semin Cancer Biol*. 1999;9(3):211-220. [CrossRef]
18. Wang Y, Xia CJ, Wang BJ, Ma XW, Zhao DW. The association between vegf -634c/g polymorphisms and osteonecrosis of femoral head: A meta-analysis. *Int J Clin Exp Med*. 2015;8(6):9313-9319.
19. Hang D, Wang Q, Guo C, Chen Z, Yan Z. Treatment of osteonecrosis of the femoral head with vegf165 transgenic bone marrow mesenchymal stem cells in mongrel dogs. *Cells Tissues Organs*. 2012;195(6):495-506. [CrossRef]
20. Yamaguchi N. An analysis of the functional mechanisms of endostatin - the anti-angiogenic activity of endostatin is mediated by its multiple binding ability. *Connect Tissue*. 2004;36(3):171-178.
21. Abdollahi A, Hlatky L, Huber PE. Endostatin: the logic of antiangiogenic therapy. *Drug Resist Updat*. 2005;8(1-2):59-74. [CrossRef]
22. Ahluwalia A, Jones MK, Deng X, Sandor Z, Szabo S, Tarnawski AS. An imbalance between vegf and endostatin underlies impaired angiogenesis in gastric mucosa of aging rats. *Am J Physiol Gastrointest Liver Physiol*. 2013;305(4):G325-G332. [CrossRef]
23. Asai K, Kanazawa H, Otani K, Shiraishi S, Hirata K, Yoshikawa J. Imbalance between vascular endothelial growth factor and endostatin levels in induced sputum from asthmatic subjects. *J Allergy Clin Immunol*. 2002;110(4):571-575. [CrossRef]
24. Nagashima M, Asano G, Yoshino S. Imbalance in production between vascular endothelial growth factor and endostatin in patients with rheumatoid arthritis. *J Rheumatol*. 2000;27(10):2339-2342.
25. Takeshita S, Kawamura Y, Takabayashi H, Yoshida N, Nonoyama S. Imbalance in the production between vascular endothelial growth factor and endostatin in Kawasaki disease. *Clin Exp Immunol*. 2005;139(3):575-579. [CrossRef]
26. Zhang C, Ma J, Li M, Li XH, Dang XQ, Wang KZ. Repair effect of coexpression of the hVEGF and hBMP genes via an adeno-associated virus vector in a rabbit model of early steroid-induced avascular necrosis of the femoral head. *Transl Res*. 2015;166(3):269-280. [CrossRef]
27. Hankenson KD, Dishowitz M, Gray C, Schenker M. Angiogenesis in bone regeneration. *Injury*. 2011;42(6):556-561. [CrossRef]
28. Grosso A, Burger MG, Lunger A, Schaefer DJ, Banfi A, Di Maggio N. It takes two to tango: coupling of angiogenesis and osteogenesis for bone regeneration. *Front Bioeng Biotechnol*. 2017;5:68. [CrossRef]
29. Yamaguchi N, Anand-Apte B, Lee M, et al. Endostatin inhibits vegf-induced endothelial cell migration and tumor growth independently of zinc binding. *EMBO J*. 1999;18(16):4414-4423. [CrossRef]
30. Holstein JH, Karabin-Kehl B, Scheuer C, et al. Endostatin inhibits callus remodeling during fracture healing in mice. *J Orthop Res*. 2013;31(10):1579-1584. [CrossRef]
31. Lazaridou M, Gkalitsiou V, Maloutas D, Volitakis A. Bevacizumab and osteonecrosis of the jaw: report of a case and review of the literature. *Hellen Arch Oral Maxillofac Surg*. 2014;15(2)77-86.
32. Wan YY, Tian GY, Guo HS, et al. Endostatin, an angiogenesis inhibitor, ameliorates bleomycin-induced pulmonary fibrosis in rats. *Respir Res*. 2013;14(1):56. [CrossRef].
33. Yamamoto T, Irisa T, Sugioka Y, et al. Effects of pulse methylprednisolone on bone and marrow tissues: corticosteroid-induced osteonecrosis in rabbits. *Arthritis Rheum*. 1997;40(11):2055-2064. [CrossRef].
34. Qin L, Zhang G, Sheng H, Yeung K, Leung K. Multiple bioimaging modalities in evaluation of an experimental osteonecrosis induced by combination of lipopolysaccharide and methylprednisolone. *Zhongguo Xiu Fu Chong Jian Wai*

Ke Za Zhi Zhongguo Xiufu Chong Jian Waike Zazhi Chin J Reparat Reconstr Surg. 2008;22(3):258-264.
35. Folkman J. Antiangiogenesis in cancer therapy–endostatin and its mechanisms of action. *Exp Cell Res*. 2006;312(5):594-607. [CrossRef]
36. Sodha NR, Clements RT, Boodhwani M, Xu SH, Sellke FW. Endostatin and angiostatin are increased in diabetic patients with coronary artery disease and associated with impaired coronary collateral formation. *AJP Heart Circ Physiol*. 2008;296(2):H428-H434.
37. Panchal VR, Rehman J, Nguyen AT, et al. Reduced pericardial levels of endostatin correlate with collateral development in patients with ischemic heart disease. *J Am Coll Cardiol*. 2004;43(8):1383-1387. [CrossRef]
38. Marneros AG, She H, Zambarakji H, Hashizume H, Olsen BR. Endogenous endostatin inhibits choroidal neovascularization. *FASEB J*. 2008;21(14): 3809-3818.
39. Bai YJ, Huang LZ, Zhou AY, Zhao M, Yu WZ, Li XX. Antiangiogenesis effects of endostatin in retinal neovascularization. *J Ocul Pharmacol Ther*. 2013;29(7): 619-626. [CrossRef]
40. Gammal SE, Moennig B, Hoffmann K, Altmeyer P. *Three-Dimensional Reconstruction of Terminal Blood Spaces in the Proximal Tibia Metaphysis of the Growing Rat — a Model to Study Normal Angiogenesis*. Springer Berlin Heidelberg; 1995.
41. Sipola A, Ilvesaro J, Birr E, et al. Endostatin inhibits endochondral ossification. *J Gene Med*. 2007;9(12):1057-1064. [CrossRef]
42. Lau KW, Kapur S, Kesavan C, Baylink DJ. Up-regulation of the wnt, estrogen receptor, insulin-like growth factor-i, and bone morphogenetic protein pathways in C57BL/6J osteoblasts as opposed to c3h/hej osteoblasts in part contributes to the differential anabolic response to fluid shear. *J Biol Chem*. 2006;281(14):9576-9588. [CrossRef]